



**ICA 2013 Montreal**  
**Montreal, Canada**  
**2 - 7 June 2013**

**Structural Acoustics and Vibration**

**Session 4aSA: Applications in Structural Acoustics and Vibration II**

## **4aSA6. Results of an implementation of the dual surface method to treat the non-uniqueness in solving acoustic exterior problems using the boundary element method**

**Ralf Burgschweiger\*, Ingo Schäfer, Adel Mohsen, Rafael Piscoya, Martin Ochmann and Bodo Nolte**

**\*Corresponding author's address: Department II, Project Group Computational Acoustics, Beuth Hochschule für Technik Berlin, University of Applied Sciences, Luxemburger Str. 10, Berlin, 13353, Berlin, Germany, [burgi@beuth-hochschule.de](mailto:burgi@beuth-hochschule.de)**

The problem of non-uniqueness (NU) of the solution of exterior acoustic problems when using the boundary element method (BEM) is well known. Methods like the Burton-Miller technique or the CHIEF method are used to solve this challenge at the expense of more complex procedures for handling hypersingular integrals and/or higher computing times due to higher complexity of the algorithm or additional equations. The dual surface method, commonly used for electromagnetic problems, was adapted for acoustic radiation and scattering problems. The basic principles of methods to solve the NU problem are outlined and results for different models and solution procedures are presented, taking into account quality, solution time and the numerical advantages when using iterative solvers.

Published by the Acoustical Society of America through the American Institute of Physics

## INTRODUCTION

The aim of this work was the benchmarking of three different methods to overcome the problem of the non-uniqueness using a mid-sized model structure under practical aspects in combination with an iterative solver. Here, the so-called Householder Version of the GMRES (Generalized Minimal Residuum, based on [1, 2]) without preconditioning was used.

The basic principles of the methods will be shown under the aspects of their computational costs; details about their mathematical principles and their implementation may be found within the cited papers.

## BASICS AND CHARACTERISTICS OF THE METHODS USED

### CHIEF Method

The CHIEF (Combined Helmholtz Integral Equation Formulation) method based on [3, 4] uses additional load points inside the structure(s), where the well known Helmholtz boundary integral equation (Eq. 1)

$$C(\vec{y}) p(\vec{y}) = \iint_S -i\omega\rho v_n(\vec{x}) g(\vec{x}, \vec{y}) dS_x - \underbrace{\iint_S p(\vec{x}) \frac{\partial g(\vec{x}, \vec{y})}{\partial n(\vec{x})} dS_x}_{\mathbf{F} \text{ coefficients}} + p_{inc}(\vec{y}) \quad (1)$$

always has a unique solution.

This leads to an overdetermined system of equations ( $\mathbf{C}_{CHIEF}$ , as shown in Fig. 1 for the rigid case).

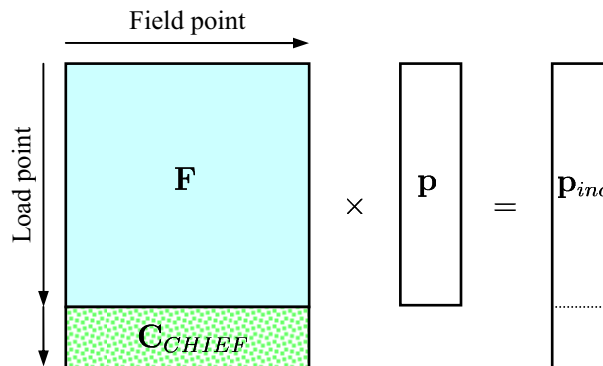


FIGURE 1. system matrix for the rigid case with additional CHIEF points

The method proposed in [5] is used to get back a quadratic form of the system matrix (Fig. 2) by using the complex conjugate values of the CHIEF matrix coefficients ( $\mathbf{C}^*$ ) and an additional unit matrix  $\mathbf{E}$  which fits better for the direct and iterative solvers used.

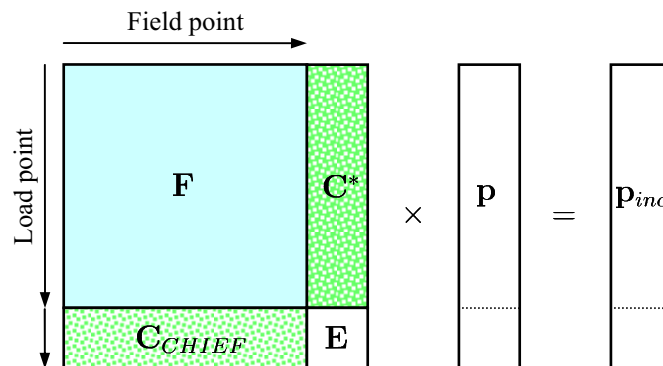


FIGURE 2. square form of the system for the rigid case with additional CHIEF points

The additional use of e.g. 10% of CHIEF points with regard to the number of elements will raise the size of the system matrix from  $N_{elem}^2$  to  $(1.1N_{elem})^2 = 1.21N_{elem}^2$ , this will increase the size of required memory and the solution time.

### Burton-Miller Method

The well-known Burton-Miller method (B&M) is based on [6] and uses a linear combination of the conventional coefficients of the Helmholtz BIE (Eq. 1) based on the fundamental solutions and their derivatives multiplied by a combination factor  $\alpha_{BM}$  (Eq. 2).

$$C(\vec{y}) [p(\vec{y}) - \alpha_{BM} i\omega\rho v_n(\vec{y})] = \iint_S -i\omega\rho v_n(\vec{x}) \left[ g(\vec{x}, \vec{y}) + \alpha_{BM} \frac{\partial g(\vec{x}, \vec{y})}{\partial n(\vec{y})} \right] dS_x - \iint_S p(\vec{x}) \left[ \frac{\partial g(\vec{x}, \vec{y})}{\partial n(\vec{x})} + \alpha_{BM} \frac{\partial}{\partial n(\vec{x})} \frac{\partial}{\partial n(\vec{y})} g(\vec{x}, \vec{y}) \right] dS_x + p_{inc}(\vec{y}) - \alpha_{BM} i\omega\rho v_{n,inc}(\vec{y}) \quad (2)$$

This leads to additional terms and raises the creation time of the system matrix, especially for the main diagonal entries where an analytical integration due to the hypersingular kernels of the second derivatives have to be used, but this does not change the matrix size. More details and some interesting examples may be found in [7].

### Dual Surface Method

The Dual Surface method (DS) was first used in the field of electromagnetic problems and adapted to exterior acoustics as shown in detail in [8]. The basic idea is to generate a virtual second surface inside the structure (Fig. 3) by shifting the original load points ( $\vec{y}$ ) along the element normal to a “virtual” surface ( $\vec{y}_{DS}$ ) using a distance  $\delta_{DS}$  which depends on the wavelength (suggestion:  $\delta_{DS} \leq \lambda/4$ ).

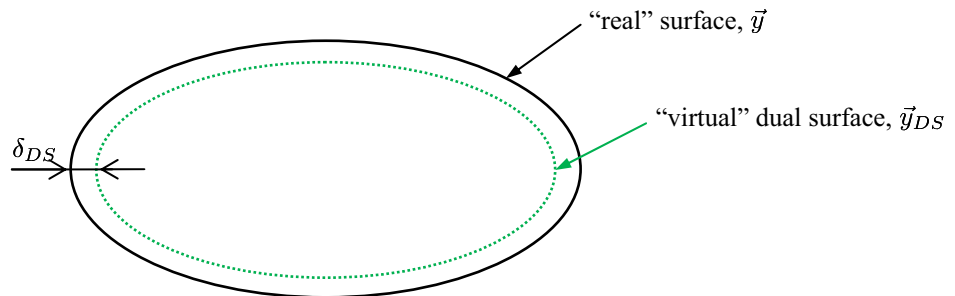


FIGURE 3. Dual Surface model scheme

This is a bit like the CHIEF method with 100% additional points but without building additional equations because the fundamental solution at these points is added to the conventional coefficients, multiplied by a combination factor  $\alpha_{DS}$ , giving a linear combination (like Burton-Miller).

$$C(\vec{y}) p(\vec{y}) = \iint_S -i\omega\rho v_n(\vec{x}) [g(\vec{x}, \vec{y}) + \alpha_{DS} g(\vec{x}, \vec{y}_{DS})] dS_x - \iint_S p(\vec{x}) \left[ \frac{\partial g(\vec{x}, \vec{y})}{\partial n(\vec{x})} + \alpha_{DS} \frac{\partial g(\vec{x}, \vec{y}_{DS})}{\partial n(\vec{x})} \right] dS_x + p_{inc}(\vec{y}) + \alpha_{DS} p_{inc}(\vec{y}_{DS}) \quad (3)$$

This will raise the creation time of the system matrix by a factor of approx. 2 but without increasing its size.

## EXAMPLE AND RESULTS

To compare the results of the different methods, a model of an ellipsoid ( $2 \times 1 \times 0.5$  m) with a small cut-out around the center as shown in Fig. 4 was used. It consists of  $N_{elem} = 26,632$  constant triangular boundary elements with a maximum element size (“border length”) of  $l_{max} = 0.031$  m which makes it suitable for frequencies up to 8 kHz in water ( $c_{water} = 1,500$  m/s,  $\lambda_{8kHz} = 0.188$  m,  $\lambda_{8kHz}/6 = 0.031$  m). A calculation was done for the rigid case using a frequency range between 100 Hz and 10 kHz in 10 Hz steps ( $N_{freq} = 991$ ) at 10 field points, which were placed around the structure, 8 in the X-Y-plane (Fig. 5) and 2 above and below the origin, using a distance of 1 km.

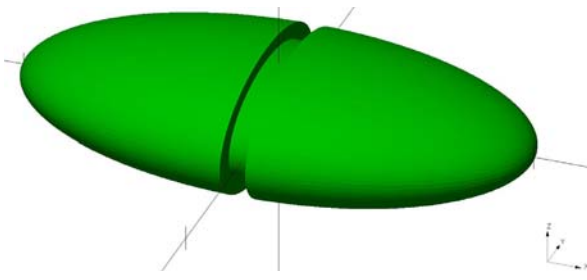


**FIGURE 4.** model of an ellipsoid with a cut-out,  $N_{elem} = 26,632$  triangles,  $l_{max} = 0.031$  m,  $l_{average} = 0.019$  m

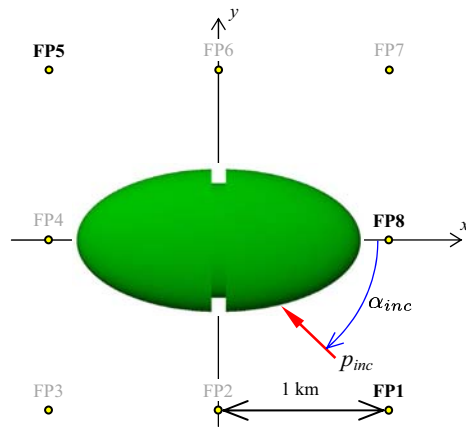


**FIGURE 5.** positions of field points,  $\alpha_{inc} = -45^\circ$

An incident plane wave hits the structure at an incident angle of  $\alpha_{inc} = -45^\circ$  which gives the chance of multiple reflections within the cut-out at higher frequencies. Additional CHIEF points (10% of  $N_{elem} = N_{CHIEF} = 2,663$ ) were placed at random positions inside the model (Fig. 6).

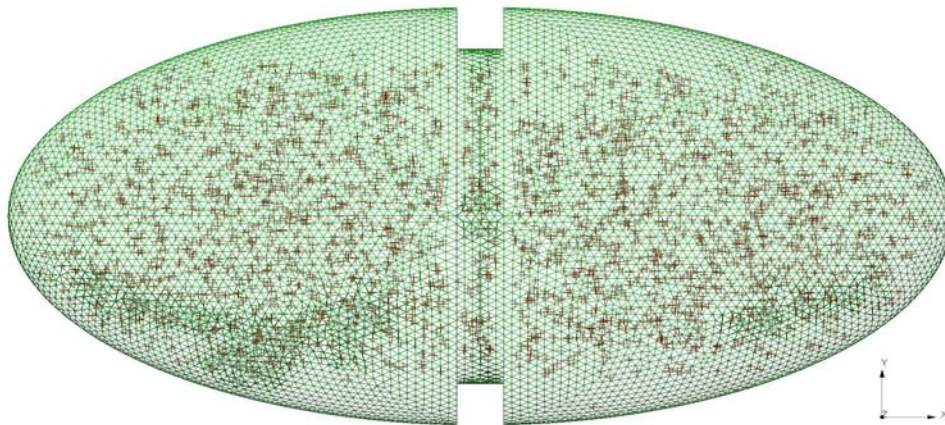


**FIGURE 6.** Top view of the mesh with  $N_{CHIEF} = 2,663$  CHIEF points placed inside the structure

All calculations were done on a Dual XEON workstation with 2,66 GHz, 12 cores and 48 GB RAM, running LINUX and using the parallelized GMRES solver of a self-developed BEM solver application code [9] which supports multiple solvers and solving methods.

The following figures (Fig. 7, 8 and 9) give the results (here: scattered pressure level) of the frequency sweep at three selected field points (FP1, FP5 and FP8). The vertical dotted blue line near 8 kHz marks the frequency limit of the used mesh with regard to the “six elements per wavelength”-rule and the maximum border length  $l_{max}$ .

All results are very similar, but above approx. 2,7 kHz one can see the first occurrences of resonances within the conventional BEM calculation without treating of the irregularities (red graph, titled “without IRT”).

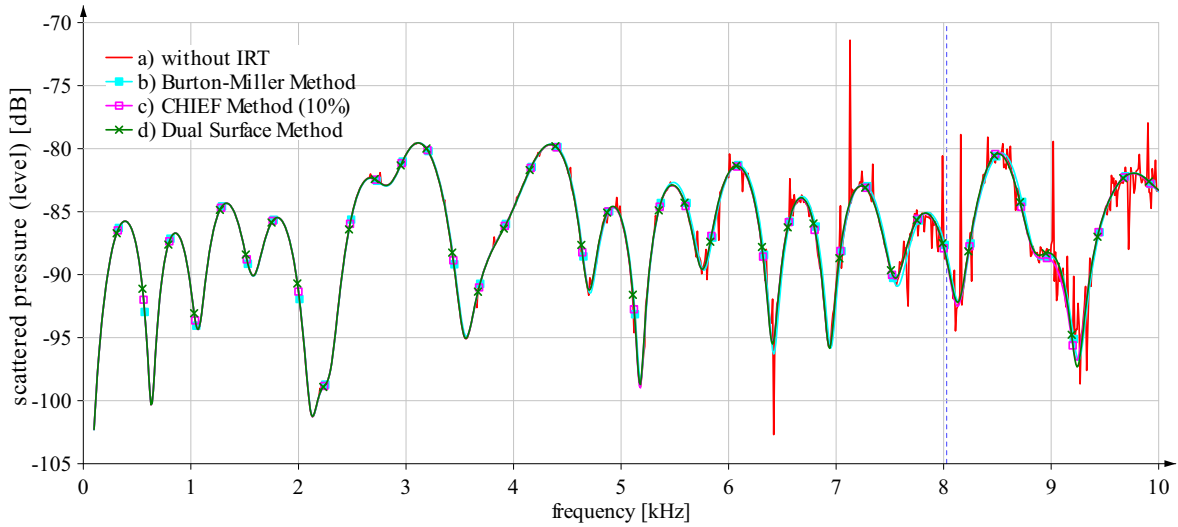


FIGURE 7. Scattered pressure level  $L_{p,scat}$  at field point FP1 [1, -1, 0] km (monostatic case)

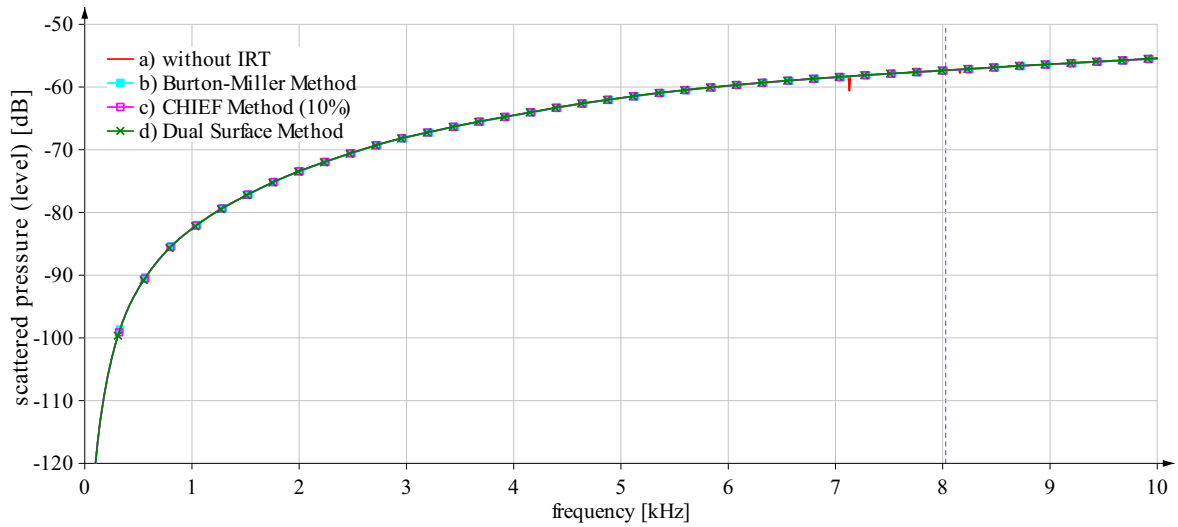


FIGURE 8. Scattered pressure level  $L_{p,scat}$  at field point FP5 [-1, 1, 0] km (shadow side, opposite to source)

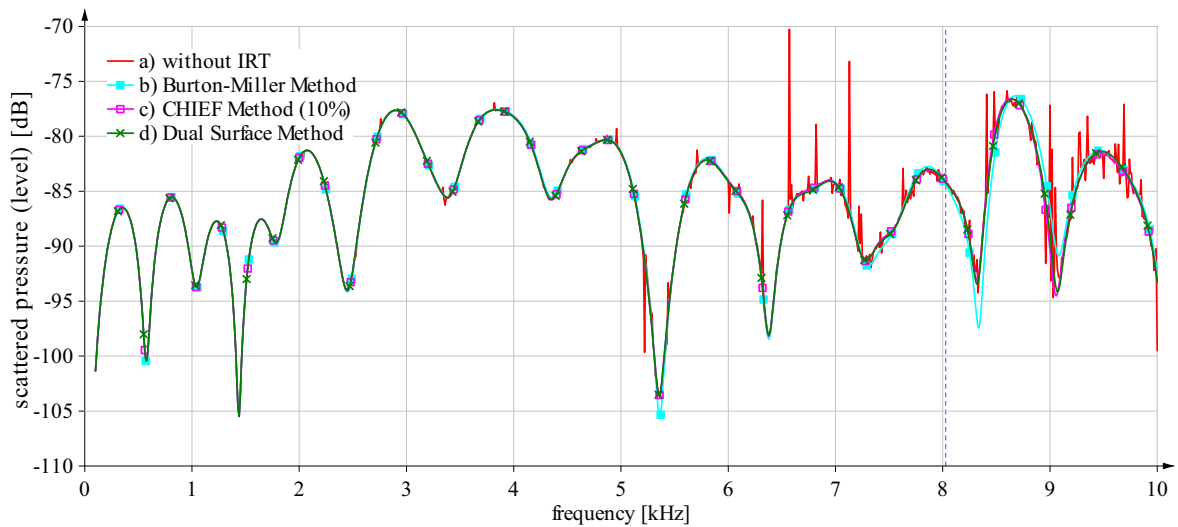


FIGURE 9. Scattered pressure level  $L_{p,scat}$  at field point FP8 [1, 0, 0] km (on positive x-axis)

All three methods used to overcome the non-uniqueness problem are in very good agreement, so one should take a look at the frequency dependent values for setting up the matrix and the solution time. With regard to the duration of the matrix setup time (Fig. 10) one can see the expected time-specific relations between the methods. The conventional BEM (without IRT) took about 20 s, the Dual Surface method nearly two times ( $\approx 38$  s), the Burton-Miller methods needs about 15% more time due to the calculation of the second derivatives and the CHIEF method requires about 20% more time for the additional equations.

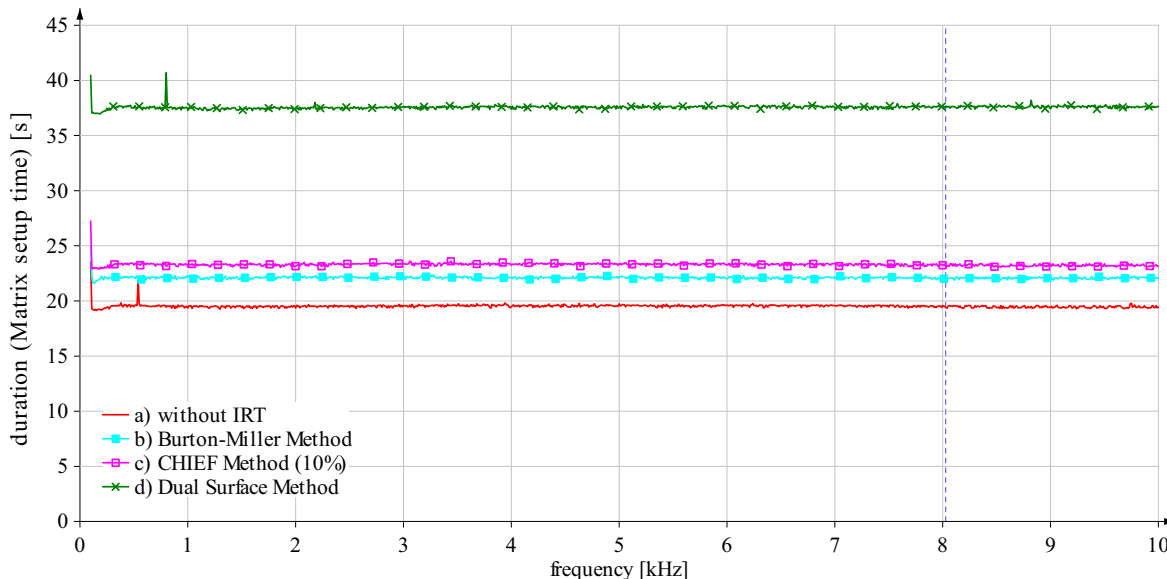


FIGURE 10. Matrix setup time

It is much more interesting to look at the number of required iterations (= number of matrix-vector-products). The number of iterations for the conventional BEM (without IRT) and the CHIEF method rises from about 10 to 500 iterations (the upper limit) to reach the given maximum relative error of  $e_{max,iter} = 10^{-4}$  (Fig. 11).

The Burton-Miller method starts with a relative high iteration number of about 100 and descends to values between 45 and 70 for higher frequencies, while the Dual Surface method, beginning with 10 and ending at 50, always has the lowest number of iterations at all frequencies.

In conclusion, both the B&M and the DS method lead to matrices with a better condition and lower iteration numbers which is very important for using iterative solvers.

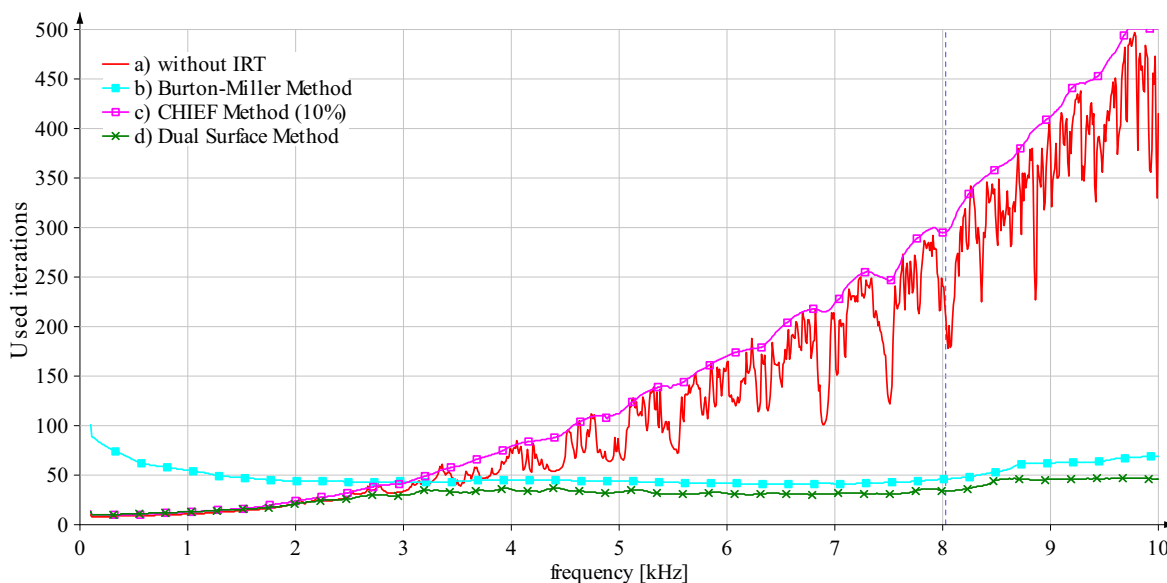


FIGURE 11. Used iterations ( $N_{max,iter} = 500$ ,  $e_{max,iter} = 10^{-4}$ )

The total solving time per frequency reflects this fact (Fig. 12). The CHIEF method leads to the largest solving times due to the higher order of the system matrix. The Burton-Miller method is at lower frequencies a little bit slower than the Dual Surface method, at higher frequencies above 2 kHz a bit faster. This difference is not very high for the example presented but we expect larger iteration numbers and solving times for the Burton-Miller method when using more complicated structures.

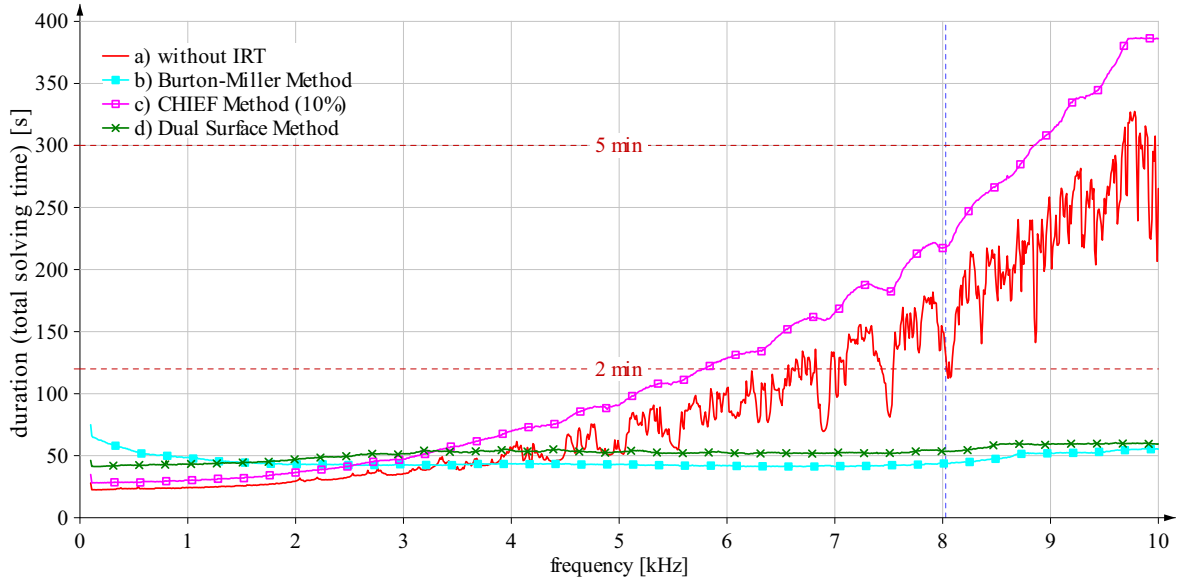


FIGURE 12. Total solving time per frequency

The following table (Tab. 1) gives the solving times for the complete frequency sweep.

TABLE 1. Solving times of the complete frequency sweep (991 frequencies)

Method	Total solving time [s]	Total solving time [h:m:s]
without IRT	95,740	26 : 35 : 40
Burton-Miller	45,202	12 : 33 : 22
CHIEF (10%)	131,722	36 : 35 : 22
Dual Surface	51,534	14 : 18 : 54
Direct solver	approx. 475.680	approx. 132 : 08 : 00

Note: The approximated time value for the direct solver is based on a one-frequency calculation using a conventional parallelized direct solver (Intel Math Kernel Library) and a matrix order of  $O_{mx} = N_{elem} = 26,632$ .

## CONCLUSIONS AND OUTLOOK

It could be shown that all three methods used to overcome the non-uniqueness problem gave similar results with regard to the quality of the solution. In combination with an iterative solver like the GMRES, the condition of the system matrix was much better for the Burton-Miller and the Dual Surface method, thus reducing the solving time significantly.

We expect that the small differences with respect to the iteration numbers for these methods for the example shown will be larger when more complicated structures will be used: thus the Dual Surface method may be chosen with preference.

Further work will be undertaken in relation to these issues and will be presented in a special paper about the Dual Surface method within the near future. Another topic of future work will be the combination of the DS method with the Multi-Level Fast Multipole Method (MLFMM) and the Source Clustering Method (SCM).

## REFERENCES

1. H. F. Walker, "Implementation of the GMRES method using householder transformations", Society of Industrial and Applied Mathematics, Journal on Scientific and Statistical Computing, Vol. 9, No. 1, 152-163 (1988)
2. Y. Saad, "Iterative Methods for Sparse Linear Systems", Society of Industrial and Applied Mathematics, Chap. 6.5, 157ff, ISBN 978-0-898715-34-7 (2003)
3. H. A. Schenck, "Improved Integral Formulation for Acoustic Radiation Problems", Journal of the Acoustical Society of America, 07/1968, Vol. 44, Issue 1, 41-58 (1968).
4. P. A. Martin, "On the Null-Field Equations for the Exterior Problems of Acoustics", Quarterly Journal of Mechanics and Applied Mathematics, Vol. 33, 385-396 (1980).
5. S. Marburg, and T. W. Wu, "Treating the Phenomenon of Irregular Frequencies", Chap. 15 in *Computational Acoustics of Noise Propagation in Fluids*, 415ff (Springer Verlag, 2008, ISBN 978-3-540-77447-1).
6. A. J. Burton and G. F. Miller, "The Application of Integral Equation Methods to the Numerical Solution of Some Exterior Boundary-Value Problems", Proc. Roy. Soc. London, A 323, 201-210 (1971)
7. A. V. Osetrov and M. Ochmann, "A Fast and Stable Numerical Solution for Acoustic Boundary Element Method Equations Combined with the Burton and Miller Method for Models Consisting of Constant Elements", Journal of Computational Acoustics, Vol. 13, 1-20 (2005).
8. A. Mohsen, R. Piscoya and M. Ochmann, "The Application of the Dual Surface Method to Treat the Nonuniqueness in Solving Acoustic Exterior Problems", Acta Acustica united with Acustica, Vol. 97, 699-707 (2011).
9. R. Burgschweiger, "Objektorientierte Implementierung eines Randelementverfahrens zur Simulation der akustischen Streuung an Objekten für ungekoppelte und gekoppelte Probleme" (Ph.D. dissertation, Technical University of Berlin, Berlin, Germany, 2012, OPUS: URN: urn:nbn:de:kobv:83-opus-34315, <http://opus.kobv.de/tuberlin/volltexte/2012/3431/>), 51ff